Metabolic responses to elevated pCO_2 in the gills of the Pacific Oyster (*Magallana gigas*) using a GC-TOF-MS-based metabolomics approach

Zengjie Jiang [1, 2], **Xiaoqin Wang** [1, 3], **Samuel P.S. Rastrick** [Corresp., 4], **Jinghui Fang** [1], **Meirong Du** [1], **Yaping Gao** [1], **Yalin Wu** [1, 3], **Øivind Strand** [4], **Jianguang Fang** [Corresp. 1, 2]

[1] Yellow Sea Fisheries Research Institute, Chinese Academy of Fishery Sciences, Qingdao, China

[2] Function Laboratory for Marine Fisheries Science and Food Production Processes, Qingdao National Laboratory for Marine Science and Technology, Qingdao, China

[3] College of Fisheries and Life Sciences, Shanghai Ocean University, Shanghai, China

[4] Institute of Marine Research, Bergen, Norway

Corresponding Authors: Samuel P.S. Rastrick, Jianguang Fang
Email address: samuel.rastrick@imr.no, Fangjg@ysfri.ac.cn

Rising atmospheric carbon dioxide (CO_2), primarily from human fossil fuel combustion and cement production, are resulting in increasing absorption of CO_2 by the oceans, which has led to a decline in ocean pH in a process known as ocean acidification (OA). There is a growing body of evidence demonstrating the potential effect of OA on life-history traits of marine organisms. Consequently, gas chromatography time-of-flight mass spectrometry (GC-TOF-MS) based metabolic profiling approach was applied to examine the metabolic responses of *Magallana gigas* to elevated pCO_2 levels, under otherwise natural field conditions. CO_2. Oysters were exposed natural environmental pCO_2 (~625.40 µatm) and elevated pCO_2 (~1432.94 µatm) levels for 30 days. Results indicated that 36 differential metabolites with variable importance in the projection (VIP) value greater than 1 and Student's t-test lower than 0.05 were identified. Differential metabolites were mapped in the Kyoto Encyclopedia of Genes and Genomes (KEGG) database to search for the related metabolic pathways. Pathway enrichment analysis indicates that alanine, aspartate and glutamate metabolism and glycine, serine and threonine metabolism were the most statistically enriched pathways. Further analysis suggested that elevated pCO_2 disturb the TCA cycle via succinate accumulation and *Magallana gigas* most likely adjust their energy metabolic via alanine and GABA accumulation accordingly to cope with elevated pCO_2. These findings provide an understanding of the molecular mechanisms involved in modulating metabolism under elevated pCO_2 levels associated with predicted OA.

Metabolic responses to elevated pCO_2 in the gills of the Pacific Oyster (*Magallana gigas*) using a GC-TOF-MS-based metabolomics approach

Zengjie Jiang [1,2], Xiaoqin Wang [1,3], Samuel P.S. Rastrick [4], Jinghui Fang [1], Meirong Du [1], Yaping Gao [1], Yalin Wu [1,3], Øivind Strand [4], Jianguang Fang [1,2]

[1] Key Laboratory of Sustainable Development of Marine Fisheries, Ministry of Agriculture, Yellow Sea Fisheries Research Institute, Chinese Academy of Fishery Sciences, Qingdao, Shandong Province, China

[2] Laboratory for Marine Fisheries Science and Food Production Processes, Qingdao National Laboratory for Marine Science and Technology, Qingdao, Shandong Province, China

[3] College of Fisheries and Life Sciences, Shanghai Ocean University, Shanghai, China

[4] Institute of Marine Research, Bergen, Norway

Corresponding Author: Jianguang Fang[1], Samuel P.S. Rastrick [2]

106 Nanjing Road, Qingdao, Shandong Province, 266071, China

NO-5817 1870 Nordnes, Bergen, Norway

Email address: fangjg@ysfri.ac.cn, samuel.rastrick@imr.no.

PeerJ Preprints | https://doi.org/10.7287/peerj.preprints.26866v1 | CC BY 4.0 Open Access | rec: 18 Apr 2018, publ: 18 Apr 2018

Abstract: Rising atmospheric carbon dioxide (CO_2), primarily from human fossil fuel combustion and cement production, are resulting in increasing absorption of CO_2 by the oceans, which has led to a decline in ocean pH in a process known as ocean acidification (OA). There is a growing body of evidence demonstrating the potential effect of OA on life-history traits of marine organisms. Consequently, gas chromatography time-of-flight mass spectrometry (GC-TOF-MS) based metabolic profiling approach was applied to examine the metabolic responses of *Magallana gigas* to elevated pCO_2 levels, under otherwise natural field conditions. CO_2. Oysters were exposed natural environmental pCO_2 (~625.40 µatm) and elevated pCO_2 (~1432.94 µatm) levels for 30 days. Results indicated that 36 differential metabolites with variable importance in the projection (VIP) value greater than 1 and Student's t-test lower than 0.05 were identified. Differential metabolites were mapped in the Kyoto Encyclopedia of Genes and Genomes (KEGG) database to search for the related metabolic pathways. Pathway enrichment analysis indicates that alanine, aspartate and glutamate metabolism and glycine, serine and threonine metabolism were the most statistically enriched pathways. Further analysis suggested that elevated pCO_2 disturb the TCA cycle via succinate accumulation and *Magallana gigas* most likely adjust their energy metabolic via alanine and GABA accumulation accordingly to cope with elevated pCO_2. These findings provide an understanding of the molecular mechanisms involved in modulating metabolism under elevated pCO_2 levels associated with predicted OA.

Keywords: Ocean acidification, *Magallana gigas*, GC-TOF-MS, metabolomics, KEGG

Introduction

Global mean atmospheric CO_2 levels have increased by more than 40% since the inception of the Industrial Revolution and are predicted to rise with an average annual increase of about 0.5%(Siegenthaler et al., 2005). Since the industrial revolution approximately one third of anthropogenic CO_2 emissions have been absorbed by the oceans, decreasing ocean surface pH by nearly 0.1 unit. This is predicted to decrease a further 0.4 units by the end of the 21st century and possibly by 0.7 pH units by 2250, in a process termed ocean acidification (OA) (Caldeira & Wickett, 2003; Orr et al., 2005).It has been suggested that progressive OA will negatively impact marine organisms, in particular calcifying organisms, by slowing calcification rates or even causing dissolution of carbonate shells when saturation states of calcite (Ω_{calc}) or aragonite (Ω_{arag}) drop below unity (Langdon et al., 2000; Hoegh-Guldberg et al., 2007; Doney et al., 2009). Additionally, increased CO_2 produces hypercapnic conditions, which have been shown to negatively affect the physiology, growth and reproductive success of marine calcifying organisms (Michaelidis et al., 2005; Berge et al., 2006; Spicer, Raffo & Widdicombe, 2007; Kurihara, 2009; Arnold et al., 2009; Cummings et al., 2011; Navarro et al., 2013).

Among calcifying species, shellfish are globally important both ecologically and as ecosystem engineers, constructing complex reef habitats and governing energy/nutrient flows in coastal ecosystems (Dumbauld, Ruesink & Rumrill, 2009; Cranford et al., 2012). With an average annual increase of 6.2% over the last 25 years, global shellfish aquaculture production reached 16.1 million tons in 2014, corresponding to a commercial value of US$ 19 billion (FAO, 2016). Oysters are one of the most important cultivated shellfish species in the world. Pacific oyster, *Magallana gigas* (formally *Crassostrea gigas*), contributed an estimated 625.93 thousand tons to global aquaculture production in 2014 (FAO, 2016). Previous studies have reported the negative impact of CO_2-driven acidification on the developmental stage and growth of *M. gigas*. For

example, studies on *M. gigas* showed a strong decrease of developmental success into viable D-shaped larvae and growth rates with increased pCO_2 (Kurihara, Kato & Ishimatsu, 2007). Barros *et al*. (2013) recorded that low values of pH decrease survival and growth rates of *M. gigas* veliger larvae, whilst increasing the frequency of prodissoconch abnormalities and protruding mantle. Gazeau *et al*. (2007) showed that the calcification rates of the Pacific oyster (*M. gigas*) decline linearly with increasing pCO_2 and oyster calcification may decrease by 10% by the end of the century. Recently, several studies have demonstrated that pCO_2 levels corresponding to predicted OA scenarios are likely to interfere with the metabolism of oysters affecting energy turnover and partitioning to production (Lannig et al., 2010; Parker et al., 2012). Reduced production as a result of global elevation in pCO_2 in this species would, not only have also major consequences for coastal biodiversity, ecosystem functioning and services, but could cause significant economic loss. Recent results show that the global economic costs of mollusk loss from OA are around 6 billion USD annually under the assumption of a constant demand and could in fact be well over 100 billion USD if the demand for mollusks increases (Narita, Rehdanz & Tol, 2012). However, the underlying mechanisms explaining oyster metabolic responses to ocean acidification remain largely unexplored.

With the development of system biology, metabolomics has recently developed and proved to be a useful tool to provide a system-wide view of understanding the complexity of metabolic networks (Nicholson, Lindon & Holmes, 1999; Gavaghan, Wilson & Nicholson, 2002; Nicholson et al., 2002; Lin, Viant & Tjeerdema, 2006; Patti, Yanes & Siuzdak, 2012; Johnson, Ivanisevic & Siuzdak, 2016). In recent years, an increasing number of studies have applied this approach to reveal the metabolic responses of organisms to environmental and anthropogenic stressors (Viant, Rosenblum & Tjeerdema, 2003; Viant 2007; Bundy, Davey & Viant, 2009; Kido Soule et al., 2015). In addition, there has been an increased application of environmental metabolomics in

studies concerning marine invertebrates (Jones et al., 2008; Tuffnail et al., 2009; Wu & Wang, 2011; Zhang et al., 2011; Kwon et al., 2012; Wu et al., 2013; Watanabe et al., 2015). However, the application of metabolomics methods to the *M. gigas* is, however, still in its infancy. Up to now, only limited studies investigated the impact of OA stress on energy metabolism and osmotic regulation of *M. gigas* using NMR-based spectroscopy (Lannig et al., 2010; Wei et al., 2015a; Wei et al., 2015b). There are various analytical platforms including liquid (LC) or gas (GC) chromatography coupled with mass spectrometry (MS), nuclear magnetic resonance spectroscopy (NMR), fourier transform infrared (FT-IR), direct infusion MS and capillary electrophoresis-MS have been developed over the past decades. Among the various approaches, GC-MS has emerged as a preferred approach based on its high sensitivity, peak resolution, reproducibility and large commercial electron ionization spectral libraries. In the present study, a GC-TOF-MS-based metabolomics approach combined with a multivariate analysis was performed to explore the physiological response in gills of *M. gigas* after the medium-term exposure to OA (30 d) stress. The findings provide new and more in-depth information for better understanding the molecular mechanisms involved in modulating *M. gigas* metabolism under elevated pCO_2.

Materials & Methods

Animal collection and acclimatization

In May 2016, experimental oysters (75.74±9.08 mm shell length, 36.51±9.38 g wet weight) were collected from a large-scale commercial oyster aquaculture area (37° 3'55.20"N, 122°32'48.08"E) in Sanggou bay, Yellow Sea, China, and transported under natural temperature conditions within 1 h of sampling to mesocosms constructed at a small semi-enclosed dock (7900 m^2 mean depth of 1.5 m.) where *M. gigas* are naturally found to a mesocosm constructed in a small semi-enclosed port (37° 2'14.71"N, 122°33'2.09"E). Two groups of 60 healthy animals were selected and individually numbered. All the animals were transferred to the mesocosm

system, where they were acclimated at ambient temperature, salinity, dissolved oxygen and pH at 19.0 °C, 32.0, 7.0-8.0 mg $O_2 \cdot L^{-1}$ and 8.0 for 2 days prior to the start of the experiment.

Experimental setup and procedure

Incubations were carried out over 30 days using *in situ* mesocosms. Six mesocosms were deployed 3 controls (pCO_2 ~625.40 µatm) and 3 elevated pCO_2 treatment (~1432.94 µatm). Each mesocosm consists of a plastic double-layer culture basket (40×30×30 cm, length×width×height) and outer net frame (1.5m×1.5m×0.3m, length×width×height) covered in net (mesh size=1 mm) which was suspended from 4 buoys with the culture basket at a depth of 50cm. Ten oysters were each placed in each culture basket. Ambient pCO_2 treatment was maintained by bubbling untreated air independently through the water in each culture basket. Elevated pCO_2 treatment was maintained by enriching the air (from a portable air pump) with CO_2 (from a CO_2 gas cylinder) in a 500ml mixing vessel (after Findlay et al., 2008; Rastrick et al., 2014). Throughout the experiment, no mortality of oysters was observed in both control and OA-stressed groups. Following the incubation, the gill tissues of three or four oysters from each culture basket were randomly sampled for metabolomics analysis. After collection, the samples were immediately frozen in liquid nitrogen immediately and stored at -80°C for later metabolite extraction.

Monitoring of the physicochemical variables of seawater

During the experiments, seawater temperature, salinity, dissolved oxygen concentration (DO) and pH in each mesocosm were measured twice a day. Seawater temperature, salinity and dissolved oxygen concentration (DO) were measured using YSI Professional Plus handheld multi-parameter water quality meter (Yellow Springs Instrument Company, USA). The pH level was measured using a commercial combination electrode (Ross type, Orion) calibrated on the U.S. National Bureau of Standards (NBS) scale. The precision of pH measurements was ± 0.001 pH units. Total alkalinity (A_T) was analysed weekly via a Metrohm 848 Titrino plus automatic

titrator (Metrohm, USA) on 100 mL GF/F filtered samples. The accuracy of measurements was ± 5 $mmol \cdot L^{-1}$. Total dissolved inorganic carbon (C_T), aqueous partial pressure of CO_2 (pCO_2), the $CaCO_3$ saturation state for calcite (Ω_{calc}) and aragonite (Ω_{arag}) were calculated with the CO2SYS Package based on the pH and total alkalinity (A_T) measurements (Table 1).

GC-TOF-MS analysis

Preparation of samples for GC-TOF-MS analysis was preformed after Cervera *et al* (2012). In brief, 50 mg of each frozen samples were extracted by 0.4mL extraction reagent with 20 μL of L-2-Chlorophenylalanine as an internal standard in a 2 mL centrifuge tube. And then, samples were vortexed for 30s and homogenized in a ball mill for 4 min at 45Hz, before being sonicated in ice-water bath for 5 min. Subsequently, the tubes were centrifuged at 13000 rpm at 4 °C for 15 min. The 0.35mL supernatant was then transferred to 2 mL GC/MS glass vials for vacuum-drying. The dried samples were dissolved and derivatized using a two-step procedure involving oximation and silyaltion before injection for GC-MS analysis.

GC-TOF-MS analysis was carried out with an Agilent 7890 gas chromatograph system coupled with a Pegasus HT time-of-flight mass spectrometer (after Ji et al., 2016). Samples (1 μL) were injected with splitless mode. The carrier gas was helium with a constant flow rate of 1mL min^{-1}. The initial temperature was heated at 50°C for 1min, then raised to 300°C at a rate of 10°C min^{-1} and maintained at 300°C for 12min. The injection, transfer line, and ion source temperatures were 280, 270, and 220°C, respectively. The mass spectrometry data were obtained at full-scan mode (m/z 50-500) at a rate of 20 spectra per second under -70eV electron impact mode. All the samples and replicates were continuously injected as one batch in random order to discriminate technical from biological variations.

Data processing and statistical analysis

Peaks were detected with Chroma TOF4.3X software (LECO Corporation, St. Joseph, MI,

USA). Metabolite annotation was carried out by LECO-Fiehn Rtx5 database using with a retention time index tolerance of 5000. All raw data were analyzed by principal component analysis (PCA) and orthogonal projection to latent structures-discriminant analysis (OPLS-DA) using SIMCA-P 14.1 software package (MKS Data Analytics Solutions, Umea, Sweden) after performing a unit variance procedure. A variable importance in projection (VIP) that exceeded 1 with a *P*-value less than 0.05 indicated the significant metabolites. In addition, Kyoto Encyclopedia of Genes and Genomes (KEGG) (http://www.genome.jp/kegg/) and NIST (http://www.nist.gov/index.html) were utilized to link these metabolites to metabolic pathways.

Results

Metabolic profiling in response to OA stress

The total ion current (TIC) chromatograms demonstrated a strong signal, large peak capacity, and reproducible retention time, indicating the reliability of metabolomic analysis. Obvious chromatographic differences were observed between different sample groups and a total of 859 peaks were assigned to compounds. By setting the threshold of spectral similarity ≥600, 158 metabolites were left through interquartile range denoising method.

The score plot of the PCA showed that samples were all lying inside the 95% confidence region (Hotelling T2 ellipse) (Fig. 1a). The results indicated an obvious separation between OA-stressed and control groups were detected. In order to obtain a higher level of group separation and get a better understanding of variables responsible for classification, OPLS-DA was used to investigate the separation further. A clear discriminability was observed between OA-stressed and control groups (Fig. 1b). Score plots based on OPLS-DA displayed significant distinct clustering trend, suggesting extensively different metabolic profiles of each intervention group (R^2Ycum= 0.99, Q^2cum= 0.761). With Q^2 intercepting the Y axis at -0.107 in the 200 random permutations test, the supervised model was considered well-guarded against overfitting.

Identification of the OA-responsive metabolites

To identify which variables were accountable for such significant separation, variable importance in the projection (VIP) values greater than 1 were considered the most relevant metabolites for explaining the responses. On the basis of the VIP>1, a total of 36 OA-responsive metabolites with significant changes (student's T-test $P<0.05$) were identified (Table 2. Among them, 4 compounds were unknown. Compared to the non-treated control group, 10 metabolites were found to be higher in OA group, while 26 were lower. Of these 32 well-identified metabolites, 7 metabolites including oleic acid, 6-phosphogluconic acid, L-malic acid, xanthurenic acid, phosphate, beta-Alanine and ornithine had VIP values above 2.0, which indicated high relevance to the difference between sample groups. Alanine, showing the greatest fold change (log2 fold change=23.43), was the gill metabolite found to be most increased in OA group compared to control and 1,3-diaminopropane was the metabolite most depleted (log2 fold change = -3.03).

Pathway mapping and metabolite-to-metabolite network construction

The 32 well-identified altered metabolites affected by OA stress were mapped to the biological pathways involved in KEGG database which were assigned to 60 pathways. Holistic pathway enrichment analysis applied by MetaboAnalyst3.0 showed that these metabolites were primarily involved in alanine, aspartate and glutamate metabolism and glycine, serine and threonine metabolism (Fig. 2).

Discussion

In this study, we report a comprehensive analysis of metabolic changes in gills of Pacific Oyster *M. gigas* responding to elevated levels of pCO_2 predicted under OA using a GC-TOF-MS-based metabolomics approach. Numerous studies have been derived for describing the physiological response of bivalves to elevated pCO_2. Few of these, however, have been

verified in the field. The experimental method used herein is based on *in situ* mesocosm experiments rather than laboratory-based measurements. The successful mesocosm approach close to "the real world" designed in the present study provides a powerful tool to link between small-scale single species laboratory experiments and observational correlative approaches applied in field surveys. The results indicated that elevated pCO_2 affects metabolite alterations. Pathway enrichment analysis revealed that two amino acid pathways (alanine, aspartate and glutamate metabolism, glycine, serine and threonine metabolism) and one carbohydrate (glyoxylate and dicarboxylate metabolism) were the most statistically enriched pathways. Among these three pathways, alanine, succinate and 4-aminobutanoate (GABA) were the significantly accumulation metabolites. Amino acids play central roles both as building blocks of proteins and as intermediates in metabolism. The 20 amino acids that are found within proteins convey a vast array of chemical versatility. However, amino acid metabolism cannot be regarded independently of carbon metabolism. Therefore, we linked the changes in amino acid levels in the present study to the carbohydrates metabolism and the TCA cycle (Fig. 3). Previous studies indicated that alanine and succinate accumulation is the indicator of anaerobic metabolism in bivalves and alanine accumulation typically precedes that of succinate (Grieshaber et al., 1994; Michaelidis et al., 2005; Kurochkin et al., 2009).

Alanine is a non-essential amino acid and plays an important role in preserving balanced levels of nitrogen and glucose in the body. Previous studies showed that the alanine fermentation would be one of the most suitable pathway to prevent pyruvate accumulation, with the additional advantage that alanine can accumulate to high concentrations without the detrimental side effects and inhibitory effects on the activities of pyruvate kinase (De Sousa & Sodek, 2003; Miyashita et al., 2007; Reggiani et al., 1998). There are two possible pathways acting as an explanation of alanine accumulation. One way is the alanine shunt where pyruvate generated from glycolysis is

193 transaminated into alanine and 2-Oxoglutarate with glutamate as amino donor. Alanine
194 accumulation has previously been reported and tend to be explained by the induction of the gene
195 expression of alanine aminotransferase (AlaAT) and an increase in the enzyme activity (Muench
196 & Good, 1994). The other way is the GABA-shunt where the synthesis of GABA from glutamate
197 followed by the production of alanine and succinic semialdehyde (Fait et al., 2008). In the present
198 study, the observed accumulation of GABA in gill of oyster under elevated pCO_2 indicates the
199 activity of a GABA shunt. However, further studies are still needed to corroborate the direct
200 evidence. Considering the conservation of lactate and ethanol levels, alanine accumulation in
201 CO_2-exposed oyster in the present study appears is likely related to alanine fermentation
202 primarily functions to regulate the level of pyruvate which being considered as the core
203 intermediate in the complex metabolic network.
204 GABA is a four-carbon non-proteinogenic amino acid and act as the major inhibitory
205 neurotransmitter in the central and peripheral nervous systems of vertebrates and in the peripheral
206 nervous system of some invertebrates (Jessen et al., 1979). The GABA accumulation has
207 previously been explained by the activation of glutamate decarboxylase (GAD) when the
208 cytosolic pH decreases (Crawford et al., 1994). The GAD-catalyzed reaction from glutamate to
209 GABA consumes H^+ and has been proposed to buffer cellular acidification during metabolic
210 oxygen limitation. It seems that the accumulation of GABA is a positive physiological response
211 when exposed to the acidify condition. However, studies have indicated that the OA-induced
212 neural signal transmission disruption through GABA-GABA receptors is directly related to the
213 behavior of the bivalves (Nilsson et al., 2012, Clements & Hunt, 2015; Peng et al., 2017).
214 Numerous studies with various species of bivalves have reported the sensitivity of the clearance
215 rate to elevated CO_2 (Fernández-Reiriz et al., 2011; Navarro et al., 2013). The GABA
216 accumulation in the gills in this study might offer a potential explanation that ocean acidification

induced Cl^- and HCO_3^- concentration changes disrupt neural signal transmissions and subsequently affect the feeding activities. To date, the potential relationship between the abnormal feeding activities and the role of GABA is not yet fully understood and requires further investigation.

Succinate is an important intermediate of the TCA cycle and plays a crucial role in generating adenosine triphosphate (ATP), also modulating energy supply for metabolism (Mills & O'Neill, 2014). Elevated succinate in the gill tissue of oysters as shown here has also been previously observed in tissue of bivalves exposed to elevated pCO_2 (Lannig et al., 2010; Ellis et al., 2014). Lannig *et al*. (2010) reported that the most notable alteration was an increase in succinate concentration during prolonged exposure to elevated CO_2 levels in the gills and hepatopancreas of *M. gigas*. Wei *et al*. (2015a) showed that the concentrations of succinate, ATP, and amino acids including arginine and lysine were significantly increased in elevated pCO_2 treated oysters *M. gigas* and suggested that increase of succinate concentration might be a bioindicator OA stress in the tissue of oysters. Succinate accumulation has previously been explained by the inhibition of succinate dehydrogenase (SDH), the enzyme responsible for the oxidization of succinate to fumarate under oxygen limitation (Rocha et al., 2010; King, Selak & Gottlieb, 2006). The other possibility of succinate accumulation can be potentially explained by activation of the GABA shunt. However, the connection between GABA and TCA cycle maybe unlikely occurred under the condition of oxygen limitation which will limit the NAD^+ supply for the reaction from GABA to succinate (Rocha et al., 2010). Moreover, decreased cytosolic pH will inhibit the activity of succinic semialdehyde dehydrogenase (SSADH) which catalysis GABA to succinate (Felle, 2005). Therefore, the GABA shunt is probably not responsible for the accumulation of succinate.

In the present study, the levels of most intermediates of the TCA cycle that we were able to determine did not change significantly under CO_2-exposure, with the clear exception of succinate

accumulation and malate decrease in combination with the alanine and GABA accumulation. This suggests that adjustments in energy metabolism previously described in *M. gigas* and other bivalves (Lannig et al., 2010; Wei et al., 2015a) possibly related to changes in energy demand and aerobic scope in response to simulated OA maybe related to alanine and GABA shunts, with disruption to the TCA cycle via succinate accumulation. Since TCA is the most crucial central pathway linking with almost all the individual metabolic pathway, the metabolic disorder of TCA cycle will likely not only inference energetic supply and demand but induce metabolic abnormalities which present an amazing complexity considering our current knowledge on the TCA cycle function and biogenesis.

Conclusions

Overall, this study has revealed the distinct metabolic profiles in gills of Pacific Oyster *M. gigas* associated with elevated pCO_2 based on *in situ* mesocosm. The results indicated that elevated pCO_2 disturb the TCA cycle via succinate accumulation and *M. gigas* most likely adjust their energy metabolic via alanine and GABA accumulation. Further investigations are needed to determine activities of key enzymes involved in TCA cycle and GABA shunt and/or metabolite fluxes to fully unravel the mechanisms of the observed metabolite shifts and their physiological consequences and triggers.

Acknowledgements

This work was supported by grants from the Central Public-interest Scientific Institution Basal Research Fund, YSFRI, CAFS (No. 20603022017019), the Director Project Financially Supported by Qingdao National Laboratory for Marine Science and Technology (No. QNLM201707), The National Natural Science Foundation of China (Nos. 41761134052, 41676147), Sino-Norway international project Environment and Aquaculture Governance (No.

83798-02), Modern Agro-industry Technology Research System (Grant No. CARS-49). The authors thank Mr. Junwei Wang, Senlin Wang and Yitao Zhang of Chudao Fisheries Corporation for their assistance through the field experiment. The authors are grateful for several anonymous reviewers whose constructive criticism improved the quality of this manuscript.

References

1. Siegenthaler U, Stocker TF, Monnin E, Luethi D, Schwander J, Stauffer B, *et al.* 2005. Stable carbon cycle–climate relationship during the late Pleistocene. *Science*, 310: 1313-1317.
2. Caldeira,K, Wickett ME. 2003. Anthropogenic carbon and ocean pH. Nature, 425: 365-365.
3. Orr JC, Fabry VJ, Aumont O, Bopp L, Doney SC, *et al*. 2005. Anthropogenic ocean acidification over the twenty-first century and its impact on calcifying organisms. *Nature,* 437: 681-686.
4. Langdon C, Takahashi T, Sweeney C, Dave C, Goddard J, Marubini F, *et al.* 2000. Effect of calcium carbonate saturation state on the calcification rate of an experimental reef. *Global Biogeochemical cycles*, 14: 639-654.
5. Hoegh-Guldberg O, Mumby PJ, Hooten AJ, Steneck RS, Greenfield P, Gomez E, *et al*. 2007. Coral reefs under rapid climate change and ocean acidification. *Science*, 318: 1737-1742.
6. Doney SC, Fabry VJ, Feely RA, Kleypas JA. 2009. Ocean acidification: the other CO_2 problem. *Annual Review of Marine Science*, 1: 169-192.
7. Michaelidis B, Ouzounis, C, Paleras A, Pörtner HO. 2005. Effects of long-term moderate hypercapnia on acid-base balance and growth rate in marine mussels *Mytilus galloprovincialis*. *Marine Ecology Progress Series*, 293:109-118.
8. Berge JA, Bjerkeng B, Pettersen O, Schaanning MT, Oxnevad S. 2006. Effects of increased

sea water concentrations of CO_2 on growth of the bivalve *Mytilus edulis* L. *Chemosphere*, 62: 681-687.

9. Spicer JI, Raffo A, Widdicombe S. 2007. Influence of CO_2-related seawater acidification on extracellular acid-base balance in the velvet swimming crab *Necora puber*. *Marine Biology*, 151: 1117-1125.
10. Kurihara H. 2009. Effects of CO_2-driven ocean acidification on the early developmental stages of invertebrates. *Marine Ecology Progress Series*, 373: 275-284.
11. Arnold KE, Findlay HS, Spicer JI, Daniels CL, Boothroyd D. 2009. Effect of CO_2- related acidification on aspects of the larval development of the European lobster, *Homarus gammarus* (L.). *Biogeosciences Discussions*, 6: 3087-3107.
12. Cummings V, Hewitt J, Van Rooyen A, Currie K, Beard S, Thrush S, *et al*. 2011. Ocean acidification at high latitudes: potential effects on functioning of the Antarctic bivalve *Laternula elliptica*. *PloS One*, 6(1): e16069.
13. Navarro JM, Torres R, Acuña K, Duarte C, Manriquez PH, Lardies M, *et al*. 2013. Impact of medium-term exposure to elevated pCO_2 levels on the physiological energetics of the mussel *Mytilus chilensis*. *Chemosphere*, 90(3): 1242-1248.
14. Dumbauld BR, Ruesink JL, Rumrill SS. 2009. The ecological role of bivalve shellfish aquaculture in the estuarine environment: a review with application to oyster and clam culture in the West Coast (USA) estuaries. *Aquaculture,* 290: 196-223.
15. Cranford PJ, Kamermans P, Krause GHM, Mazurie J. 2012. An ecosystem-based approach and management framework for the integrated evaluation of bivalve aquaculture impacts. *Aquaculture Environment Interactions*, 2: 193-213.
16. FAO. 2016. The State of World Fisheries and Aquaculture 2016. Contributing to food security and nutrition for all. Rome. 200 pp.

313 17. Kurihara H, Kato S, Ishimatsu A. 2007. Effects of increased seawater pCO_2 on early
314 development of the oysters *Crassostrea gigas*. *Aquatic Biology*, 1: 91-98.
315 18. Barros P, Sobral P, Range P, Chícharo L, Matias D. 2013. Effects of sea-water acidification
316 on fertilization and larval development of the oyster *Crassostrea gigas*. *Journal of Marine*
317 *Biology and Ecology*, 440: 200-206.
318 19. Gazeau F, Quiblier C, Jansen JM, Gattuso JP, Middelburg JJ, Heip CHR. 2007. Impact of
319 elevated CO_2 on shellfish calcification. *Geophysical Research Letters*, 34(7): L07603.
320 20. Lannig G, Eilers S, Pörtner HO, Sokolova IM, Bock C. 2010. Impact of ocean acidification
321 on energy metabolism of Oyster, *Crassostrea gigas*-Changes in metabolic pathways and
322 thermal response. *Marine Drugs*, 8: 2318-2339.
323 21. Parker LM, Ross P, O'Connor W, Borysko L, Raftos DA, Pörtner HO. 2012. Adult exposure
324 influences offspring response to ocean acidification in oysters. *Global Change Biology*,
325 18:82-92. doi: 10.1111/j.1365-2486.2011.02520.x.
326 22. Narita D, Rehdanz K, Tol RSJ. 2012. Economic costs of ocean acidification: a look into the
327 impacts on global shellfish production. *Climatic Change*, 113(3): 1049-1063.
328 23. Nicholson JK, Lindon JC, Holmes E. 1999. 'Metabolomics': understanding the metabolic
329 responses of living systems to pathophysiological stimuli via multivariate statistical analysis
330 of biological NMR spectroscopic data. *Xenobiotica*, 29: 1181-1189.
331 24. Gavaghan CL, Wilson ID, Nicholson JK. 2002. Physiological variation in metabolic
332 phenotyping and functional genomic studies: use of orthogonal signal correction and
333 PLS-DA. *Febs Letters*, 530: 191-196.
334 25. Nicholson JK, Connelly J, Lindon JC, Holmes E. 2002. Metabolomics: a platform for
335 studying drug toxicity and gene function. *Natural Reviews Drug Discovery*, 1: 153-161.
336 26. Lin CY, Viant MR, Tjeerdema RS. 2006. Metabolomics: methodologies and applications in

337 the environmental sciences. *Journal of Pesticde Science*, 31: 245-251.
338 27. Patti GJ, Yanes O, Siuzdak G. 2012. Innovation: Metabolomics: The apogee of the omics
339 trilogy. *Nature. Reviews. Molecular Cell Biology*, 13: 263-269.
340 28. Johnson CH, Ivanisevic J, Siuzdak G. 2016. Metabolomics: beyond biomarkers and towards
341 mechanisms. *Nature Reviews Molecular Cell Biology*, 17:
342 451-459.doi:10.1038/nrm.2016.25.
343 29. Viant MR, Rosenblum ES, Tjeerdema RS. 2003. NMR-based metabolomics: a powerful
344 approach for characterizing the effects of environmental stressors on organism health.
345 *Environmental Science Technology,*37: 4982-4989.
346 30. Viant MR. 2007. Metabolomics of aquatic organisms: the new 'omics' on the block. *Marine*
347 *Ecology Progress Series*, 332: 301-306.
348 31. Bundy J, Davey M, Viant M. 2009. Environmental metabolomics: a critical review and
349 future perspectives. *Metabolomics*, 5: 3-21.
350 32. Kido Soule MC, Longnecker K, Johnson WM, Kujawinski EB. 2015. Environmental
351 metabolomics: Analytical strategies. *Marine Chemistry*, 177(Part 2): 374-387.
352 33. Jones OAH, Dondero F, Viarengo A, Griffin JL. 2008. Metabolic profiling of Mytilus
353 galloprovincialis and its potential applications for pollution assessment. *Marine Ecology*
354 *Progress Series*, 369: 169-179.
355 34. Tuffnail W, Mills GA, Cary P, Greenwood R. 2009. An environmental ^{1}H NMR
356 metabolomic study of the exposure of the marine mussel *Mytilus edulis* to atrazine, lindane,
357 hypoxia and starvation. *Metabolomics*, 5: 33-43.
358 35. Wu H, Wang WX. 2011. Tissue-specific toxicological effects of cadmium in green mussels
359 (*Perna viridis*): nuclear magnetic resonance-based metabolomics study. *Environmental.*
360 *Toxicology and Chemistry*, 30: 806-812.

361 36. Zhang LB, Liu XL, You LP, Zhou D, Wu HF, Li LZ, Zhao JM, Feng JJ, Yu JB. 2011.
362 Metabolic responses in gills of Manila clam *Ruditapes philippinarum* exposed to copper
363 using NMR-based metabolomics. *Marine Environmental Research*, 72(1-2): 33-39.
364 37. Kwon YK, Jung YS, Park JC, Seo J, Choi MS, Hwang GS. 2012. Characterizing the effect of
365 heavy metal contamination on marine mussels using metabolomics. *Marine Pollution*
366 *Bulletin*, 64: 1874-1879.
367 38. Wu HF, Zhang XY, Wang Q, Li LZ, Ji CL, Liu XL, Zhao JM, Yin XL. 2013. A metabolomic
368 investigation on arsenic-induced toxicological effects in the clam *Ruditapes philippinarum*
369 under different salinities. *Ecotoxicology and Environmental Safety*, 90(3): 1-6.
370 39. Watanabe M, Meyer KA, Jackson TM, Schock TB, Johnson WE, Bearden DW. 2015.
371 Application of NMR-based metabolomics for environmental assessment in the Great Lakes
372 using zebra mussel (*Dreissena polymorpha*). *Metabolomics,* 11: 1302-1315.
373 doi:10.1007/s11306-015-0789-4.
374 40. Wei L, Wang Q, Wu HF, Jia CL, Zhao JM. 2015a. Proteomic and metabolomic responses of
375 Pacific oyster *Crassostrea gigas* to elevated pCO_2 exposure. *Journal of proteomics*, 112:
376 83-94.
377 41. Wei L, Wang Q, Ning XX, Mu CK, Wang CL, Cao RW, *et al*. 2015b. Combined metabolome
378 and proteome analysis of the mantle tissue from Pacific oyster *Crassostrea gigas* exposed to
379 elevated pCO_2. *Comparative Biochemistry and Physiology, Part D: Genomics and*
380 *Proteomics*, 13:16-23.
381 42. Findlay HS., Kendall MA, Spicer JI, Turley C, Widdicombe S. 2008. A novel microcosm
382 system for investigating the impacts of elevated carbon dioxide and temperature on marine
383 organisms. *Aquatic Biology*, 3: 51-62.
384 43. Rastrick SPS, Calosi P, Calder-Potts R, Foggo A, Nightingale G, Widdicombe S, Spicer JI.

2014. Living in warmer, more acidic oceans retards physiological recovery from tidal emersion in the velvet swimming crab, *Necora puber*. *The Journal of Experimental Biology*, 217: 2499-2508.

44. Cervera MI, Portolés T, Pitarch E, Beltrán J, Hernández F. 2012. Application of gas chromatography time-of-flight mass spectrometry for target and non-target analysis of pesticide residues in fruits and vegetables. *Journal of Chromatography A*, 1244:168-177.
45. Ji J, Sun JD, Pi FW, Zhang S, Sun C, Wang XM, Zhang YZ, Sun XL. 2016. GC-TOF/MS-based metabolomics approach to study the cellular immunotoxicity of deoxynivalenol on murine macrophage ANA-1 cells. *Chemico-Biological Interactions*, 256: 94-101.
46. Pierrot D, Lewis E, Wallace DWR. 2006. MS Excel Program Developed for CO_2 System Calculations.
47. Mehrbach C, Culberson CH, Hawley JE, Pytkowicz RM. 1973. Measurement of the apparent dissociation constants of carbonic acid in seawater at atmospheric pressure. *Limnology and Oceanography*, 18: 897-907.
48. Dickson AG, Millero FJ. 1987. A comparison of the equilibrium constants for the dissociation of carbonic acid in seawater media. *Deep-Sea Research*, 34: 1733-1743.
49. Grieshaber MK, Hardewig I, Kreutzer U, Poertner HO. 1994. Physiological and metabolic responses to hypoxia in invertebrates. *Reviews of Physiology Biochemistry and Pharmacology*, 125: 143-147.
50. Michaelidis B, Ouzounis C, Paleras A, Pörtner HO. 2005. Effects of long-term moderate hypercapnia on acid-base balance and growth rate in marine mussels *Mytilus galloprovincialis*. *Marine Ecology Progress Series*, 293:109-118.
51. Kurochkin IO, Ivanina AV, Eilers S, Downs CA, May LA, Sokolova IM. 2009. Cadmium

affects metabolic responses to prolonged anoxia and reoxygenation in eastern oysters *Crassostrea virginica*. *American Journal of Physiology*, R1262-R1272.

52. De Sousa CAF, Sodek L. 2003. Alanine metabolism and alanine aminotransferase activity in soybean (*Glycine max*) during hypoxia of the root system and subsequent return to normoxia. *Environmental and Experimental Botany*, 50: 1-8.
53. Miyashita Y, Dolferus R, Ismond KP, Good AG. 2007. Alanine aminotransferase catalyses the breakdown of alanine after hypoxia in Arabidopsis thaliana. *Plant Journal*, 49: 1108-1121.
54. Reggiani R, Cantu´ CA, Brambilla I, Bertani A. 1998. Accumulation and interconversion of amino acids in rice roots under anoxia. *Plant and Cell Physiology,* 29: 981-987.
55. Muench DG, Good AG. 1994. Hypoxically inducible barley alanine aminotransferase: cDNA cloning and expression analysis. *Plant Molecular Biology*, 24: 417-427.
56. Fait A, Fromm H, Walter D, Galili G, Fernie AR. 2008. Highway or byway: the metabolic role of the GABA shunt in plants. *Trends in Plant Science*, 13: 14-19.
57. Jessen KR, Mirsky R, Dennison ME, Burnstock G. 1979. GABA may be a neurotransmitter in the vertebrate peripheral nervous system. *Nature*, 281: 71-74.
58. Crawford LA, Bown AW, Breitkreuz KE, Guinel FC. 1994. The synthesis of γ-aminobutyric acid in response to treatments reducing cytosolic pH. *Plant Physiology*, 104: 865-871.
59. Nilsson GE, Dixson DL, Domenici P, McCormick MI, Sørensen C, Watson S-A, Munday PL. 2012. Near-future carbon dioxide levels alter fish behaviour by interfering with neurotransmitter function. *Nature Climate Change*, 2: 201-204.
60. Clements JC, Hunt HL. 2015. Marine animal behaviour in a high CO_2 ocean. *Marine Ecology Progress Series*, 536: 259-279.
61. Peng C, Zhao XG, Liu SX, Shi W, Han Y, Guo C, Peng X, Chai XL, Liu GX. 2017. Ocean

433 acidification alters the burrowing behaviour, Ca^{2+}/Mg^{2+}-ATPase activity, metabolism, and
434 gene expression of a bivalve species, *Sinonovacula constricta*. *Marine Ecology Progress*
435 *Series*, 575: 107-117.
436 62. Fernández-Reiriz MJ, Range P, Álvarez-Salgado XA, Labarta U. 2011. Physiological
437 energetics of juvenile clams Ruditapes decussatus in a high CO_2 coastal ocean. *Marine*
438 *Ecology Progress Series*, 433: 97-105.
439 63. Navarro JM, Torres R, Acuña K, Duarte C, Manriquez PH, Lardies M, Lagos NA, Vargas C,
440 Aguilera V. 2013. Impact of medium-term exposure to elevated pCO_2 levels on the
441 physiological energetics of the mussel *Mytilus chilensis*. *Chemosphere*, 90: 1242-1248.
442 64. Mills E, O'Neill LA. 2014. Succinate: a metabolic signal in inflammation. *Trends in Cell*
443 *Biology*, 24(5): 313-320.
444 65. Ellis RP, Spicer JI, Byrne JJ, Sommer U, Viant MR, White DA, Widdicombe S. 2014. ^1H
445 NMR metabolomics reveals contrasting response by male and female mussels exposed to
446 reduced seawater pH, increased temperature, and a pathogen. *Environmental Science and*
447 *Technology*, 48: 7044-7052.
448 66. Rocha M, Licausi F, Araújo WL, Nunes-Nesi A, Sodek L, Fernie AR, van Dongen JT. 2010.
449 Glycolysis and the tricarboxylic acid cycle are linked by alanine aminotransferase during
450 hypoxia induced by waterlogging of *Lotus japonicus*. *Plant Physiology*, 152(3): 1501-1513.
451 67. King A, Selak MA, Gottlieb E. 2006. Succinate dehydrogenase and fumarate hydratase:
452 linking mitochondrial dysfunction and cancer. *Oncogene*, 25: 4675-4682.
453 68. Felle HH. 2005. pH regulation in anoxic plants. *Annals of Botany*, 96: 519-532.

Figure 1(on next page)

Score plots of PCA (a) and OPLS-DA (b) for OA-stressed (red) and control (black) groups

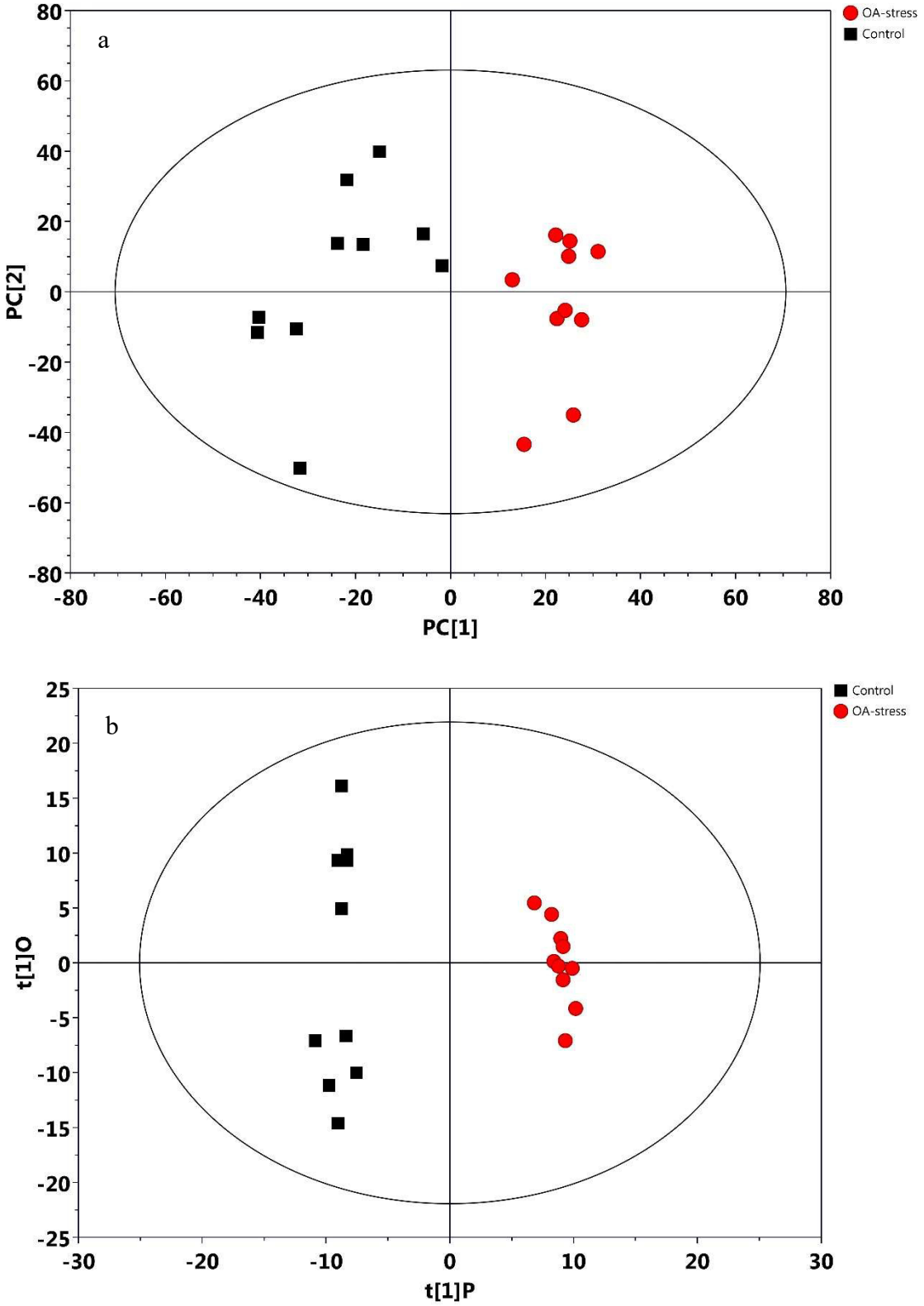

Fig.1 Score plots of PCA (a) and OPLS-DA (b) for OA-stressed (red) and control (black) groups

Figure 2(on next page)

Pathway enrichment analysis of the altered metabolites upon OA stresses exposure

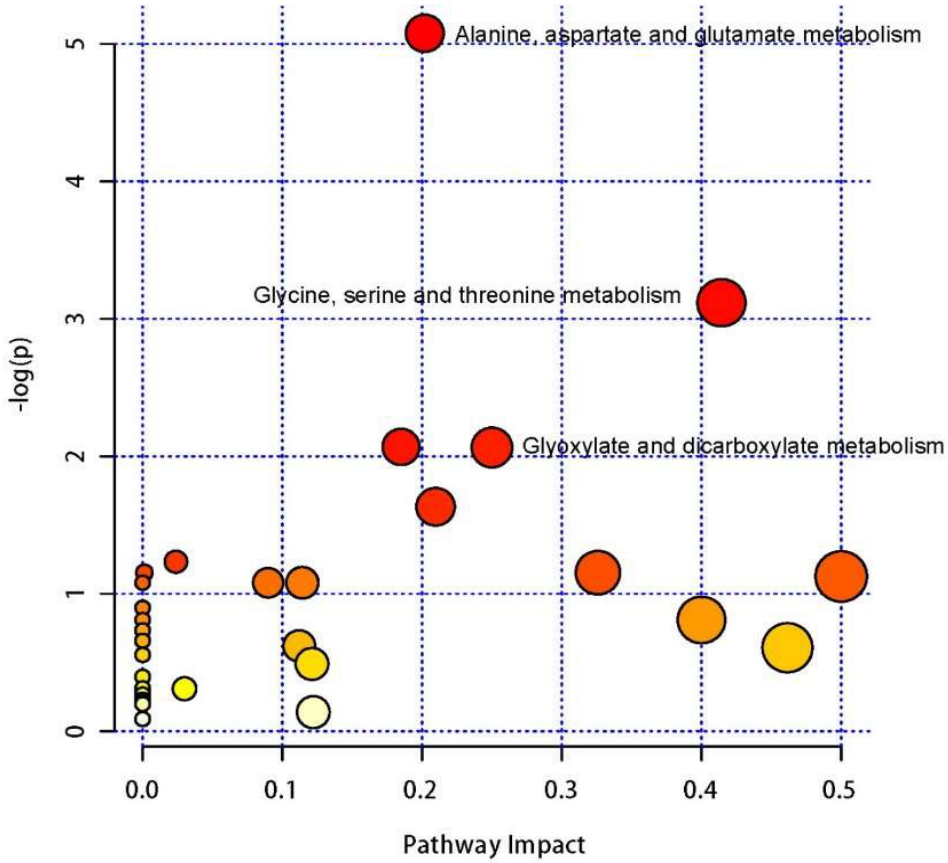

Fig 2. Pathway enrichment analysis of the altered metabolites upon OA stresses exposure.

Figure 3(on next page)

Response of metabolism pathways to OA stress in gills of oyster

The metabolites colored with red and blue indicate the up- and down-regulated ($P < 0.05$) metabolites respectively

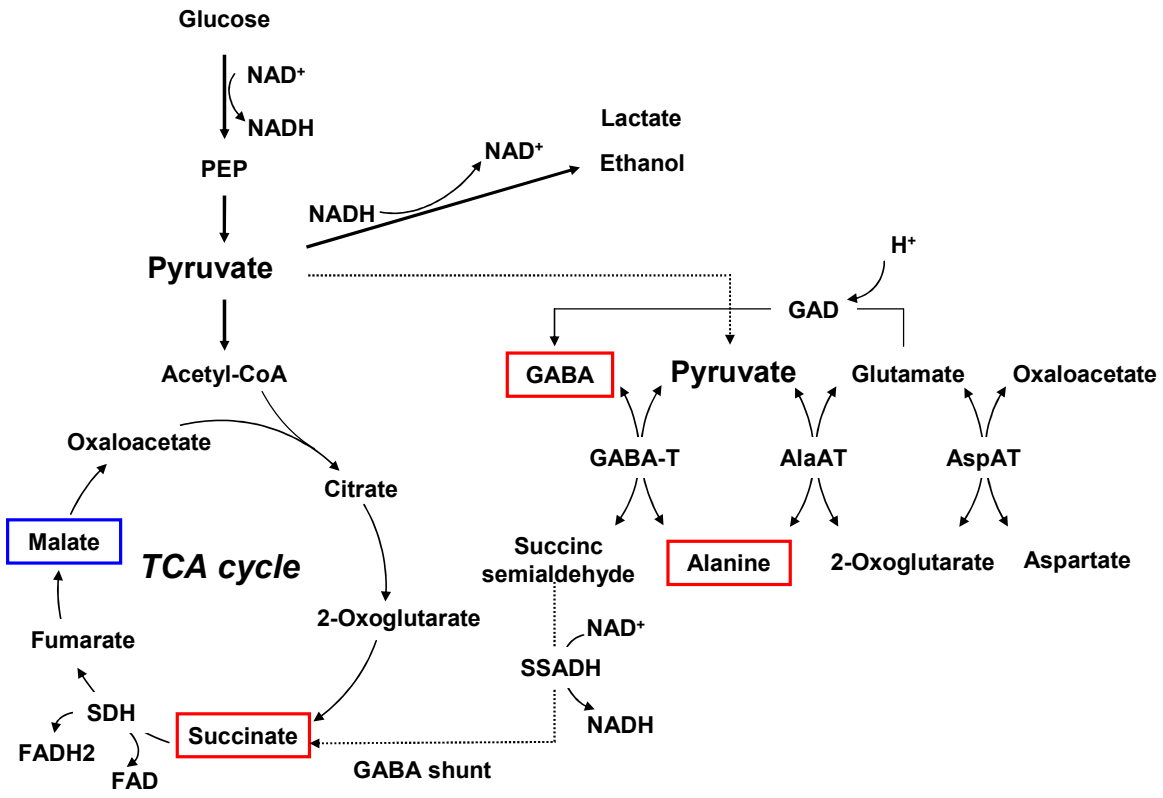

Fig 3. Response of metabolism pathways to OA stress in gills of oyster. The metabolites colored with red and blue indicate the up- and down-regulated ($P < 0.05$) metabolites respectively.

Table 1(on next page)

Summary of the OA-responsive metabolites with significant changes derived from GC-TOF-MS analysis

Table 1. Seawater chemistry variables over the 30 days experimental period

	Control pH_{NBS} 8.0	Low pH_{NBS} 7.7
Measured		
Temperature(℃)	19.08±2.06^{A}	19.09±1.95^{A}
Salinity	32.07±0.48^{A}	32.09±0.43^{A}
pH_{NBS}	7.97±0.15^{A}	7.68±0.17^{B}
A_T (μmol kg^{-1})	2211.53±92.72^{A}	2206.00±77.74^{A}
Calculated		
C_T(μmol kg^{-1})*	2081.88±34.39	2169.69±50.28
pCO_2(μatm)	625.40±21^{A}	1432.94±27^{B}
Ω_{calc}	2.61±0.32	1.43±0.30
Ω_{arag}	1.68±0.20	0.92±0.19
HCO_3^- (μmol kg^{-1})	1950.93±38.64	2060.67±48.29
CO_3^{2-} (μmol kg^{-1})	106.79±12.90	58.77±12.30

Temperature, salinity and pH_{NBS} scale were measured three times a day. Total alkalinity (A_T) was measured weekly. All other parameters [pCO_2; calcite and aragonite saturation state (Ω_{calc} and Ω_{arag}, respectively); HCO_3^-; and CO_3^{2-}] were calculated from pH_{NBS} and A_T with CO2SYS (Pierrot, Lewis & Wallace, 2006) using the dissociation constants of Mehrbach *et al*. (1973) as refitted by Dickson and Millero (1987). Values are means ± SD. Different letters indicate significant variation between treatments (ANOVA, $P < 0.05$).

Table 2(on next page)

Summary of the OA-responsive metabolites with significant changes derived from GC-TOF-MS analysis

Table 2. Summary of the OA-responsive metabolites with significant changes derived from GC-TOF-MS analysis

Peak	Similarity	R.T.	VIP	p-value	q-value	log2 fold change
Oleic acid	894	22.8515,0	2.66	0.00	0.01	22.20
6-phosphogluconic acid	716	24.4599,0	2.52	0.00	0.00	-1.33
L-Malic acid	929	15.1303,0	2.41	0.00	0.01	-2.17
Xanthurenic acid	903	23.2262,0	2.33	0.00	0.00	-2.17
Phosphate	866	12.3447,0	2.12	0.01	0.04	3.02
Beta-Alanine	935	14.433,0	2.05	0.00	0.00	-1.21
Unknown	794	10.1494,0	2.05	0.01	0.03	-1.69
Ornithine	891	18.964,0	2.00	0.00	0.00	-1.29
1,2,4-Benzenetriol	713	16.5623,0	1.91	0.00	0.00	-1.07
Unknown	694	18.1099,0	1.85	0.00	0.00	-2.41
Alpha-D-glucosamine 1-phosphate	677	19.073,0	1.82	0.00	0.02	-1.05
Alanine	918	9.87567,0	1.75	0.03	0.06	23.43
O-Phosphorylethanolamine	937	18.5929,0	1.72	0.00	0.00	-0.96
Unknown	657	19.7691,0	1.69	0.00	0.00	-2.12
L-Allothreonine	950	13.8234,0	1.69	0.00	0.02	-0.71
Conduritol b epoxide	733	20.2858,0	1.63	0.00	0.02	-1.18
Methyl-beta-D-galactopyranoside	824	19.2909,0	1.59	0.00	0.02	-0.87
Alpha-Aminoadipic acid	660	17.8244,0	1.59	0.00	0.01	-2.24
Cytidine-monophosphate	664	20.9698,0	1.56	0.02	0.05	-0.91
Lysine	899	20.0334,0	1.53	0.02	0.04	-1.05
Serine	926	13.4789,0	1.51	0.00	0.02	-0.78
Galactose	878	19.7292,0	1.50	0.00	0.02	2.32
Myristic Acid	904	19.3209,0	1.50	0.02	0.05	-0.60
O-Phosphoserine	773	19.1044,0	1.45	0.00	0.00	-2.49
Ribose-5-phosphate	892	21.7439,0	1.42	0.00	0.01	-1.25
Pyrogallol	792	15.8774,0	1.40	0.01	0.03	-0.91
Unknown	702	23.8081,0	1.40	0.04	0.07	-2.73
4-aminobutyric acid	766	15.7454,0	1.36	0.03	0.06	1.86
Maltose	919	26.9238,0	1.31	0.02	0.05	1.78
Lactose	732	26.7022,0	1.29	0.03	0.07	1.99
Ciliatine	862	18.175,0	1.24	0.01	0.04	-0.74
1,3-diaminopropane	729	17.138,0	1.22	0.01	0.03	-3.03
21-hydroxypregnenolone	651	29.4326,0	1.20	0.04	0.08	0.40
Succinic acid	868	12.8776,0	1.07	0.00	0.01	1.94
1,5-Anhydroglucitol	676	19.4587,0	1.05	0.05	0.09	3.32
Cycloleucine	706	13.6351,0	1.05	0.02	0.05	-0.91